SMART ANTENNA FOR BRAIN TUMOUR APPLICATION

By

BALAJI.R (211715106018)
BALAJI.V (211715106019)
BUVANESH.G (211715106022)
IV year, ECE,

UNDER THE GUIDANCE OF
Mrs.S.Kalaivani, M.E.,
Asst.Prof,
ECE, Dept.,

Introduction

- Brain tumour is one of the most dangerous diseases that may affect the life of the human.
- According to the statistics, 13.2 million deaths of tumour are expected in 2030.
- Brain tumour is malignant or benign mass or growth of abnormal cells in the brain.
- Magnetic Resonance Imaging (MRI), it is more dangerous for patients as it increase the cancer risk and it is very expensive.
- In Computed Tomography (CT) scan there is a risk to patient because of high ionizing radiation dose and it is also very expensive.
- Specific Absorption rate technique mainly concentrate on the absorption rate between the healthy and defected brain cells. Also SAR based techniques are accurate, cost effective.

Objective

- To design and fabricate the Microstrip Patch antenna for the desired frequency range of 2.4 – 2.7GHz.
- To analyse the Specific Absorption Rate from the obtained parameters, in order to detect the presence of tumour we model the head phantom with tumour and without tumour with the help of CST software.

Literature Review

S.NO	TITLE	YEAR	AUTHOR NAME	JOURNAL NAME	REMARKS
1	**UWB Antenna for Brain stroke and Brain Tumour Detection**	2016	M.A. Shokry, Prof. Dr.A.M. M.A. Allam	Electromagnetic field computation (IEEE)	✓ There is a good agreement between the measured and simulated results of the return loss of the antenna on human's head and head phantom. × We can only detect the presence of brain tumour with radius 24.6mm and above.

Literature Review

S.NO	TITLE	YEAR	AUTHOR NAME	JOURNAL NAME	REMARKS
2	**An Antenna for Microwave Brain Imaging**	2015	Adhitya Satria Pratama, Basari*, Muhammad Firdaus S. Lubis, Fitri Yuli Zulkifli, Eko Tjipto Rahardjo	Antennas and Propagation (IEEE)	✓ This antenna is a printed dipole fed by a coplanar waveguide it provides high frequency response × The entire desired working frequencies can be covered by adding perturbation on antenna structure.

Literature Review

S.NO	TITLE	YEAR	AUTHOR NAME	JOURNAL NAME	DEMERITS
3	**Optimization of Vivaldi Antenna for Tumour Detection**	2013	Mohammed A. Alzabidi, Maged A. Aldhaeebi and Ibrahim Elshafiey	Artificial Intelligence, Modelling & Simulation (IEEE)	✓ The antenna is immersed in background of relative permittivity 40 to achieve good matching with the head tissue. Results show that good performance is obtained. × With the increase of frequency of operation, the resolution is enhanced, while the energy penetration is reduced. There is thus a trade-off between these two.

Literature Review

S.NO	TITLE	YEAR	AUTHOR NAME	JOURNAL NAME	REMARKS
4	**Microwave Imaging for Brain Tumour Detection Using an UWB Vivaldi Antenna Array November**	2012	Haoyu Zhang, Brian Flynn, Ahmet T. Erdogan, Tughrul Arslan	Loughborough Antennas & Propagation (IEEE)	✓ The impulse intensity is employed to represent the tumour location since the antenna array rotates 1.5° for each step which offers enough precision for image processing. × Antenna array rotates far away from the tumour, only a few sets of data can be collected since the tumour reflections are very weak around there.

Literature Review

S.NO	TITLE	YEAR	AUTHOR NAME	JOURNAL NAME	REMARKS
5	**A Smart Antenna Array for Brain Cancer Detection**	2011	Haoyu Zhang, Ahmed O. El-Rayis, Nakul Haridas, Nurul H. Noordin, Ahmet T. Erdogan, Tughrul Arslan	Loughborough Antennas & Propagation (IEEE)	✓ The antenna array is composed of three ultra-wideband Vivaldi antennas which have relatively small dimensions and provide good performance. × The response of brain with tumor and without tumour have similar profile only amplitude of brain with tumour is slightly greater than others.

EXISTING MODEL

- An UWB Pentagon antenna is designed to detect brain stroke and brain tumour. It is operating at a band from 3.3568-12.604 GHz in free space and from 3.818 to 9.16 GHz on the normal head model.
- The head phantom with conductivity and permittivity as that of the human head was analysed by the signal transmitted and received from the antenna.

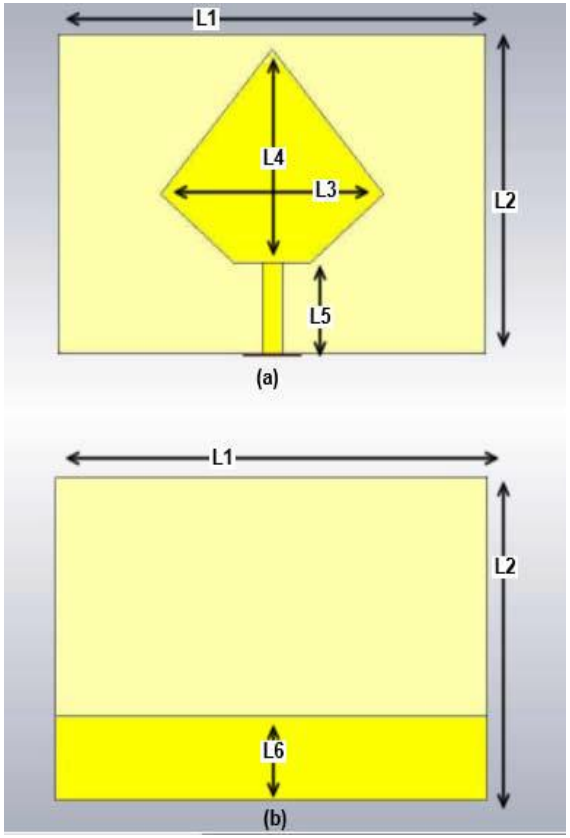

Existing Model

- It is an Microstrip Patch Antenna with very high Operating frequency 3.3568-12.604 GHz in free space and from 3.818 to 9.16 GHz on the normal head model.
- This may cause the patient headache and nausea.
- The antenna is also complex to design and operate.

Proposed Model

- A Microstrip patch antenna, was designed and simulated on the CST Microwave Studio.
- The free space testing was done with the designed antenna and its S-Parameter, gain were measured.
- Then an head phantom model which is having the conductivity and permittivity same as that of the human’s head was designed using the CST 2018 software.

Flow Chart of Proposed Model

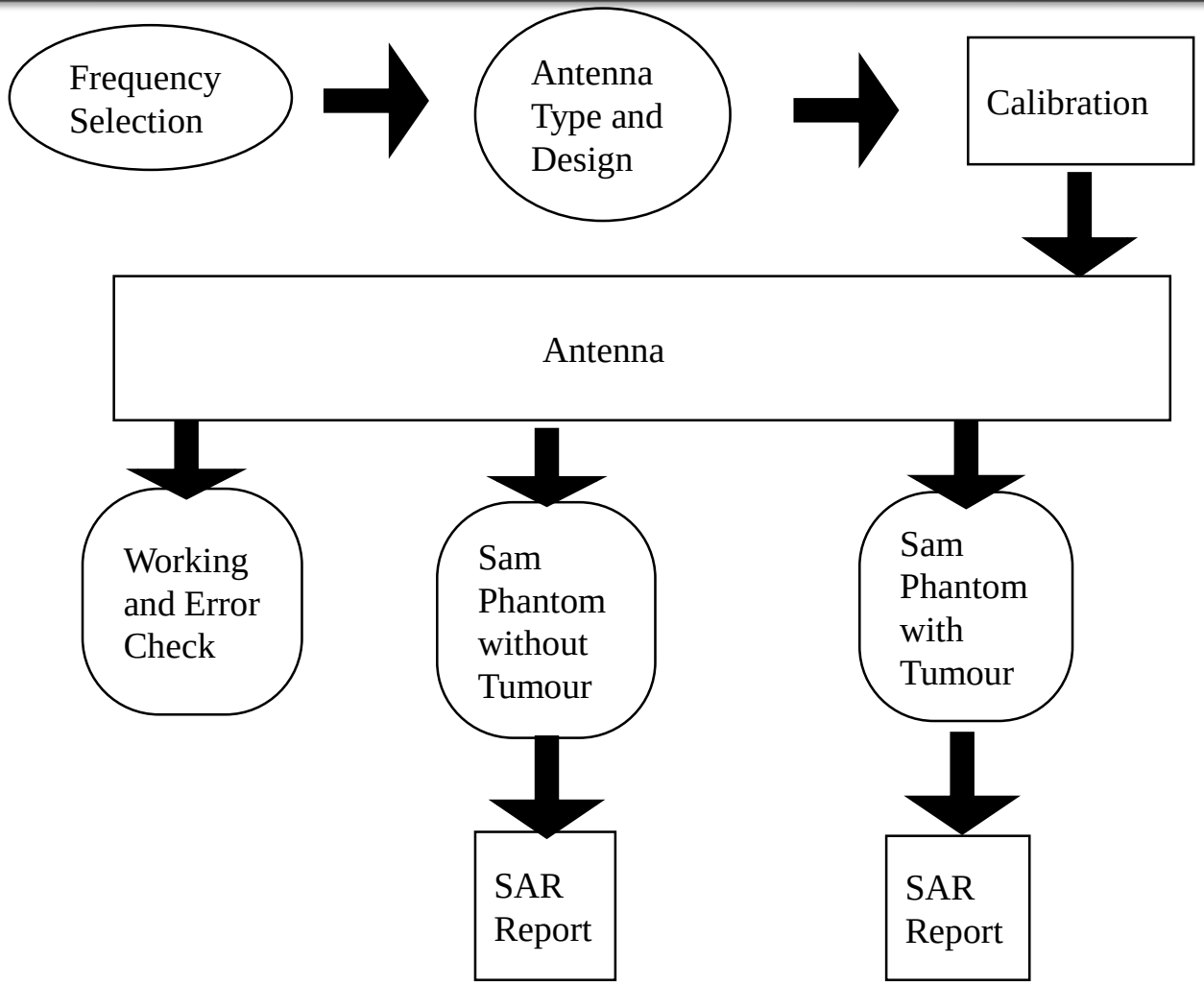

Frequency Selection

- The operating frequency of our antenna is around 2.4GHz to 2.7 GHz.
- Its is a low gain antenna with a gain of -10dB gain at 2.55GHz of frequency.

Antenna Type and Design

- The antenna used here is a Microstrip Patch antenna which is made up of Copper and Stainless steel because of its cost efficient property.
- The antenna is designed in the form of “E”, “B” and “G”.
- The feed given to this antenna is co-axial feed which is the commonly used feeding method and the most effective one in microstrip patch antenna.
- The total length and breath of the antenna is 50x50mm and thickness is 2mm.

Antenna Type and Design Cont.,

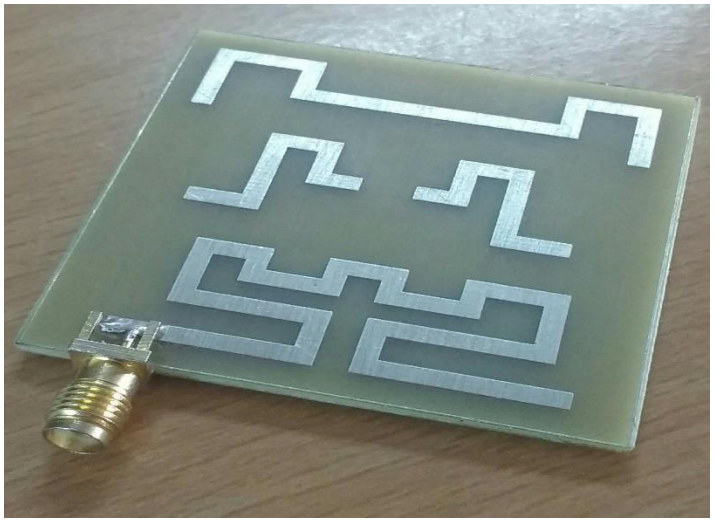

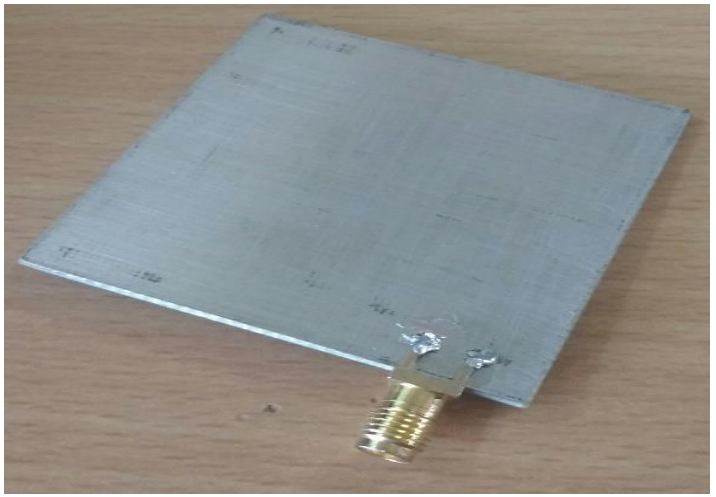

Patch	Length (mm)
E	169
B	39
G	82

Calibration

- This method is done in hardware to ensure that there is no error in the Network Analyzer to which the Microstrip antenna is connected through the feeding point. There are three different components in it they are,
  - Load,
  - Short,
  - Open.

Calibration Cont.,

Calibration	Resistance (ohms)
Load	50
Short	0
Open	infinite

Working and Error Check

- Before working with human head model, the antenna is checked for zero error and if the error is found the error is eliminated using bit error rate.

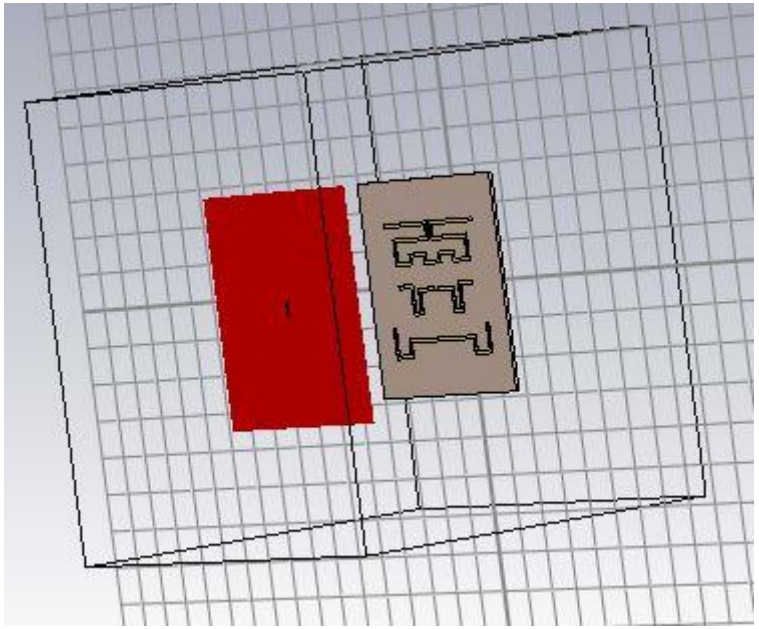

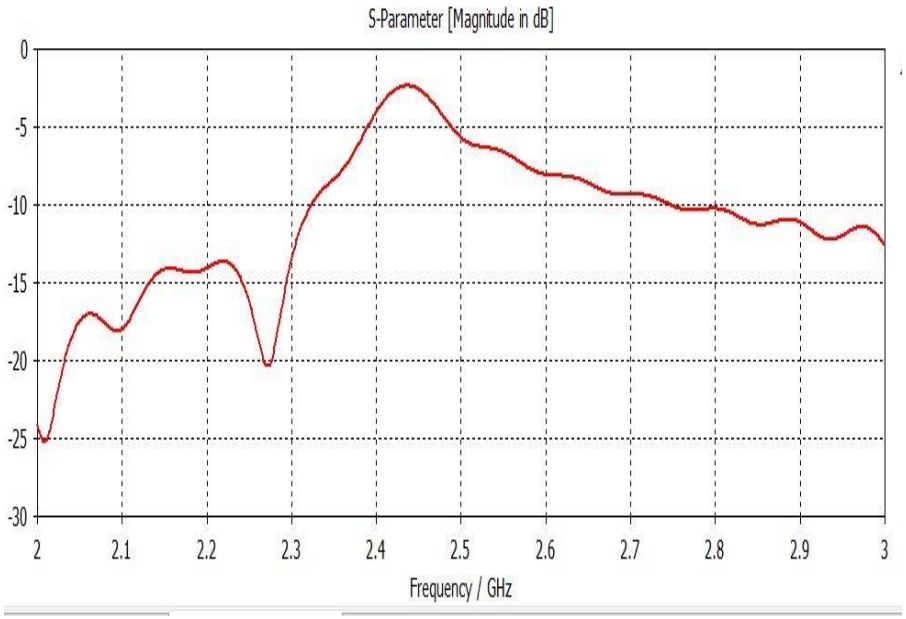

Working and Error Check Hardware

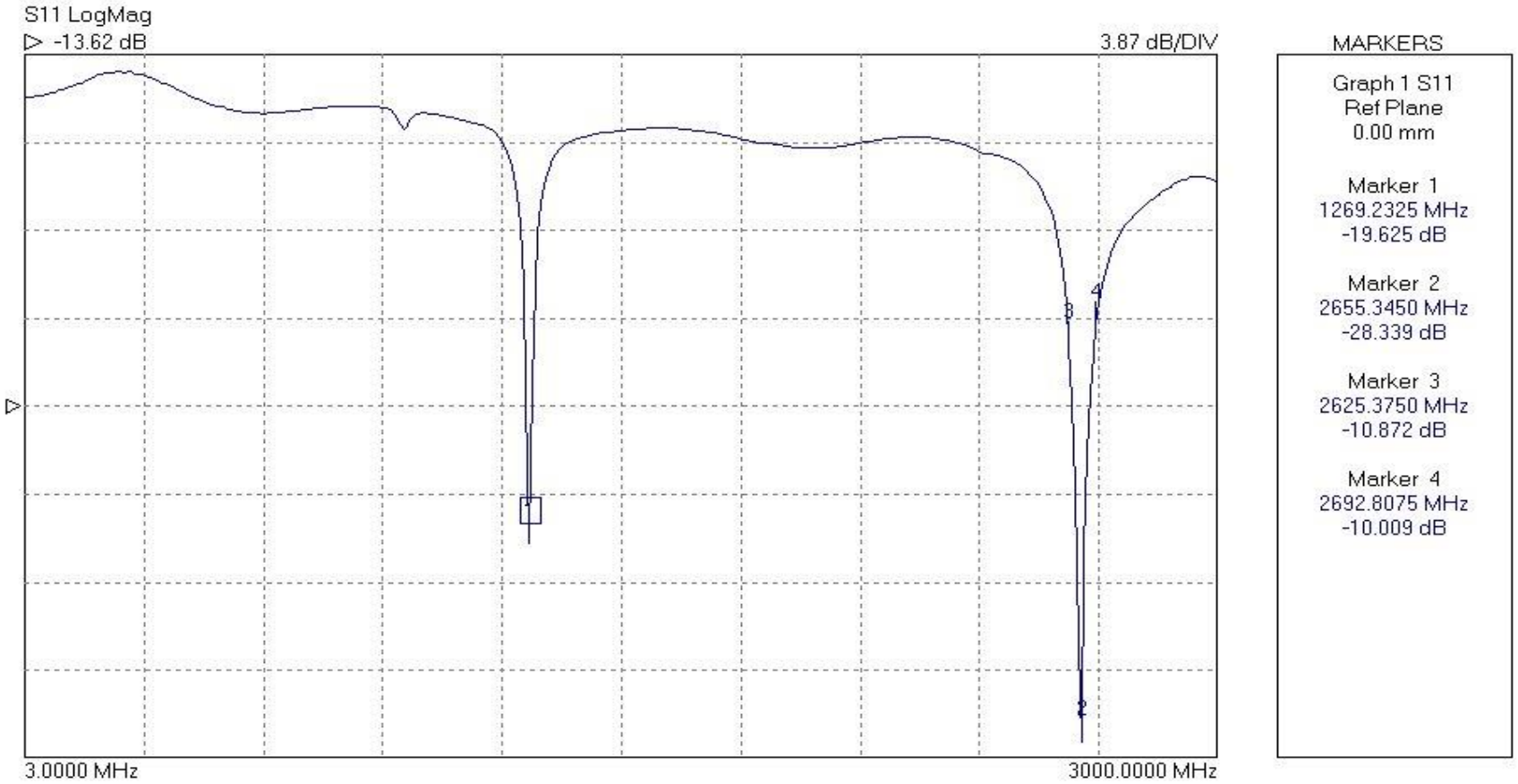

Working and Error Check Software

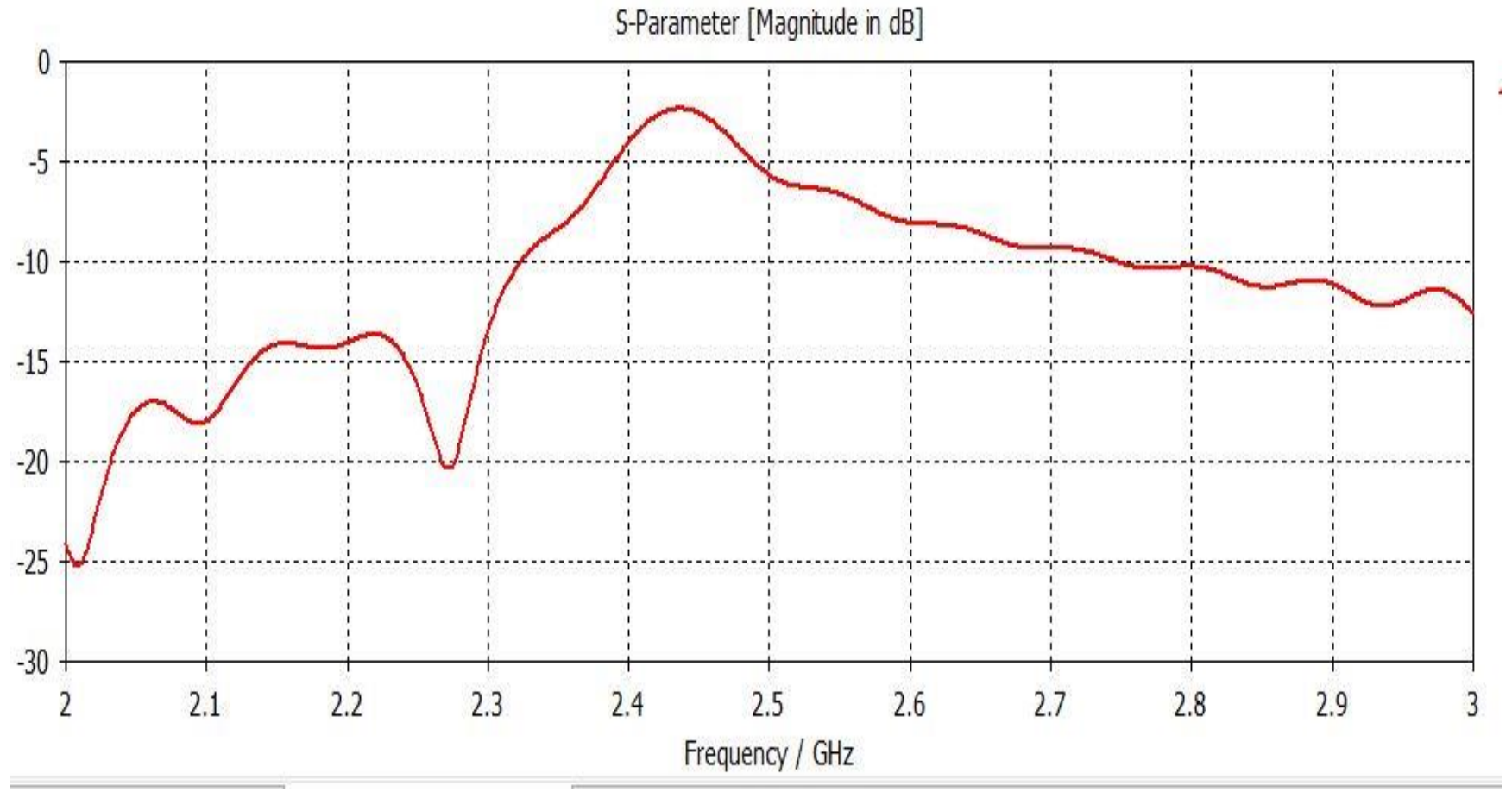

Sam Phantom without Tumour

- Here the antenna is placed at a distance of 60mm or 6 cm because the most effective radiance distance covered by it is at 60mm from the antenna. This helps the SAR calculation to have a maximum SAR point of 1.6W/kg or above which is widely required for the detection of Brain tumour in the human head.

Sam Phantom without Tumour

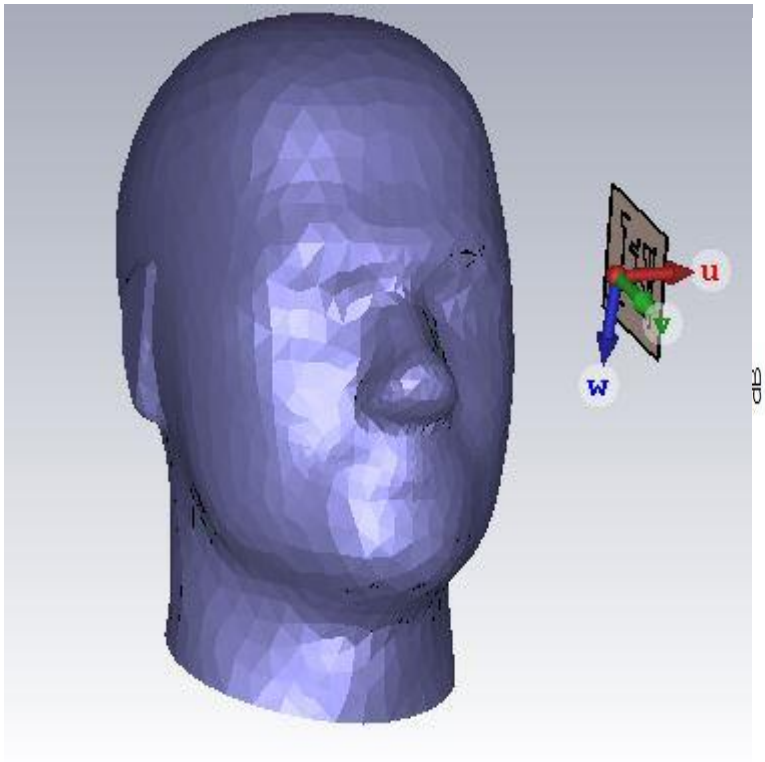

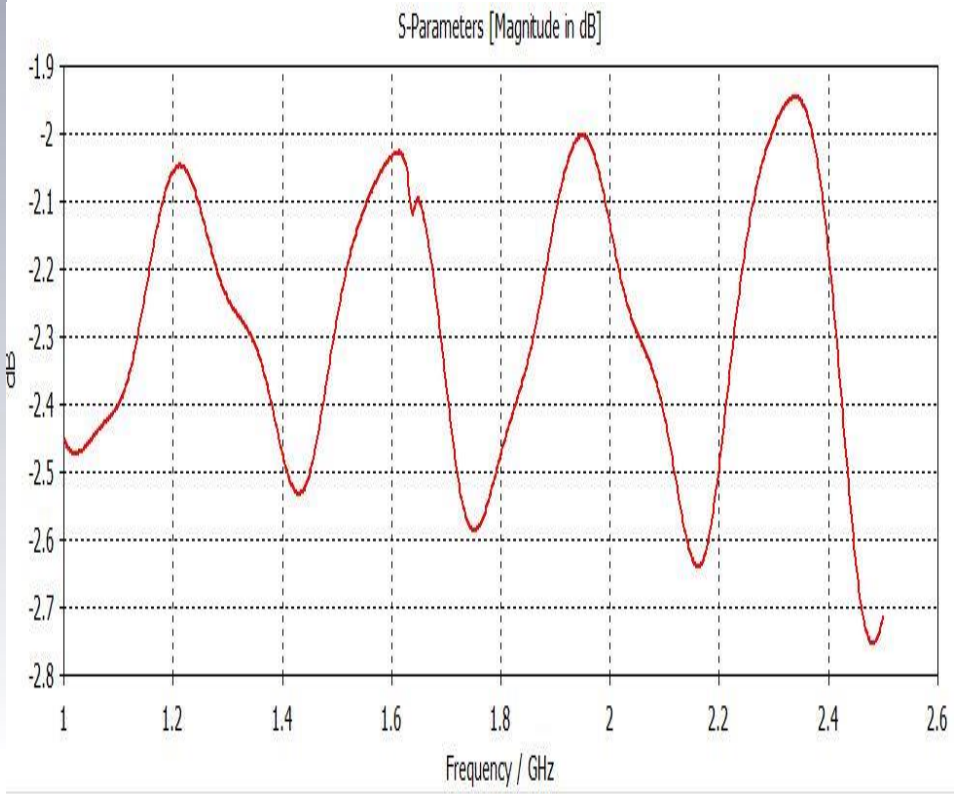

Sam Phantom with Tumour

- Here the antenna is placed at a distance of 60mm or 6 cm because the most effective radiance distance covered by it is at 60mm from the antenna. This helps the SAR calculation to have a maximum SAR point of 1.6W/kg below which is widely required for the detection of Brain tumour in the human head.
- The tumour used here is a tissue collective.

Sam Phantom with Tumour

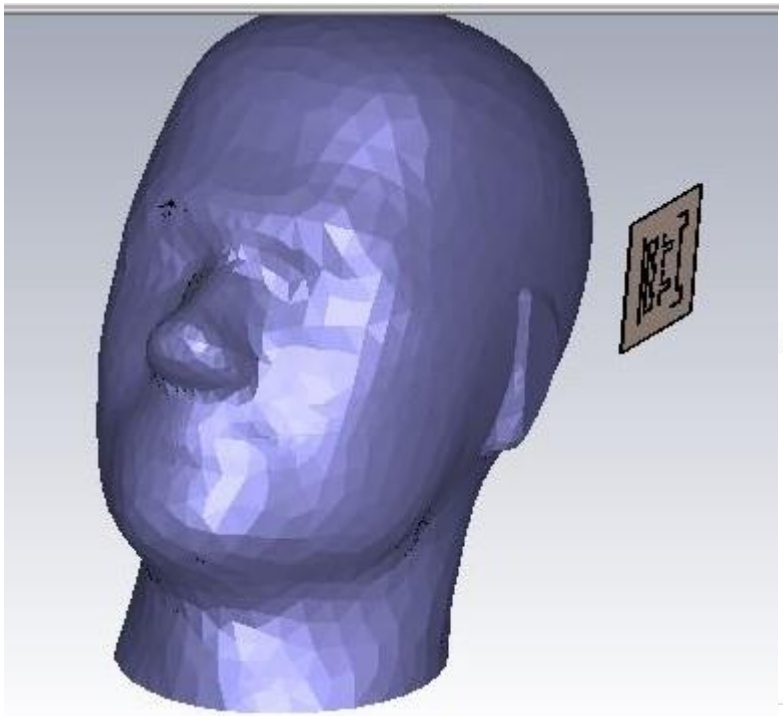

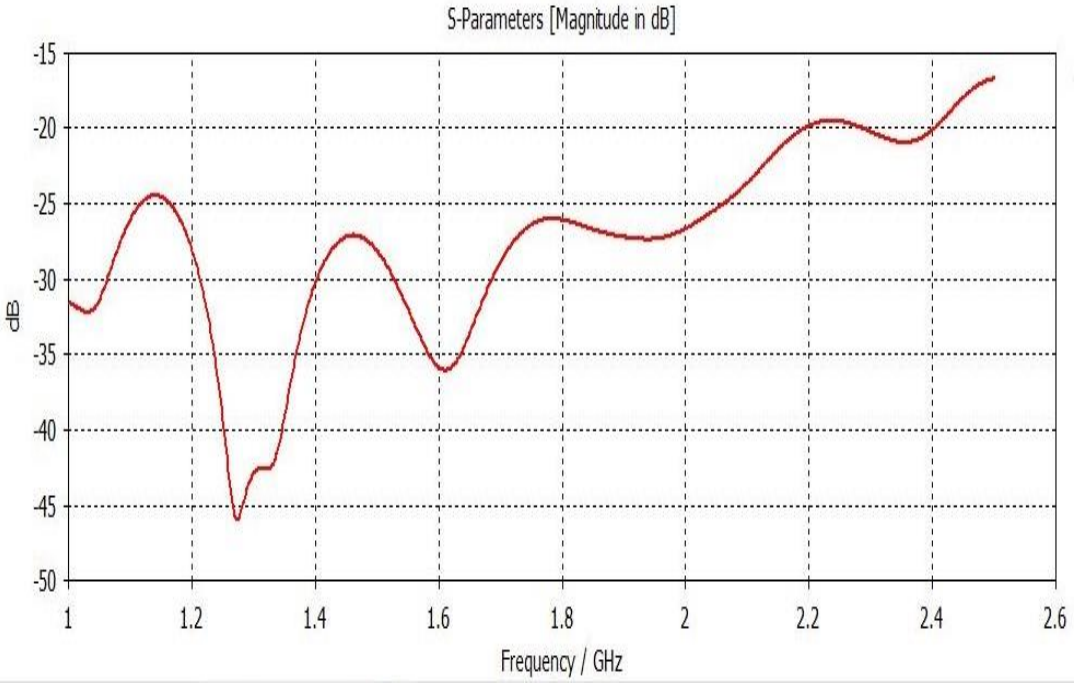

Experimental results and discussion

- The SAR Specific Absorption Rate is the main parameter we required to identify the presence of tumour in the brain.
- As we start the stimulation we can get the SAR Report after completion of the process.

Sam Phantom without Tumour

Powerloss density monitor used: loss (f=3.25) [1] at 3.25 GHz
Power scaling [W] : None
Stimulated Power [W] : 0.5
Accepted Power [W] : 0.495295
Average cell mass [g]: 0.239004
Averaging method: IEEE/IEC 62704-1
Averaging mass [g]: 10

Entire Volume:

Min (x,y,z) [mm]: -458.62, -474.741, -774.741
Max (x,y,z) [mm]: 833.36, 774.741, 474.741
Volume [mm^3]: 2.22313e+009
Absorbed power [W]: 9.91352e-008
Tissue volume [mm^3]: 5.24992e+006
Tissue mass [kg]: 5.24992
Tissue power [W]: 8.46537e-008
Average power [W/mm^3]: 1.61248e-014
Total SAR [W/kg]: 1.61248e-008
Max. point SAR [W/kg]: 1.67883e-005

Maximum SAR (10g) [W/kg]: 2.3938e-007
Maximum at (x,y,z) [mm]: 41.9061, 95.1025, 3.88218
Avg.vol.min (x,y,z) [mm]: 28.7336, 81.93, -15.9941
Avg.vol.max (x,y,z) [mm]: 55.0786, 108.275, 10.3509
Largest valid cube [mm]: 24.6852
Smallest valid cube [mm]: 21.5443
Avg.Vol.Accuracy [%]: 0.01

Calculation time [s]: 2

This is the SAR Specific Absorption Rate report of Sam Phantom with tumour which shows the Max. SAR point in around 1.6 W/Kg

Sam Phantom with Tumour

Powerloss density monitor used: loss (f=2.7) [1] at 2.7 GHz
Power scaling [W] : None
Stimulated Power [W] : 0.5
Accepted Power [W] : 0.499974
Average cell mass [g]: 0.0543158
Averaging method: IEEE/IEC 62704-1
Averaging mass [g]: 10

Entire Volume:

Min (x,y,z) [mm]: -458.62, -474.741, -774.741
Max (x,y,z) [mm]: 833.36, 774.741, 474.741
Volume [mm^3]: 2.13909e+009
Absorbed power [W]: 3.01756e-005
Tissue volume [mm^3]: 5.24992e+006
Tissue mass [kg]: 5.25
Tissue power [W]: 2.87697e-005
Average power [W/mm^3]: 5.48003e-012
Total SAR [W/kg]: 5.47995e-006
Max. point SAR [W/kg]: 0.00610628

Maximum SAR (10g) [W/kg]: 5.57132e-005
Maximum at (x,y,z) [mm]: 72.3735, 109.285, -155.927
Avg.vol.min (x,y,z) [mm]: 58.8969, 95.8084, -157.738
Avg.vol.max (x,y,z) [mm]: 85.8501, 122.762, -130.785
Largest valid cube [mm]: 23.6305
Smallest valid cube [mm]: 21.4984
Avg.Vol.Accuracy [%]: 0.01

Calculation time [s]: 12

This is the SAR Specific Absorption Rate report of Sam Phantom with tumour which shows the Max. SAR point in less than 1.6 W/Kg

Conclusion

- The human head phantom is designed with and without tumour, tested with the proposed antenna. The various response (with and without tumour) observed by the antenna and analyzed using CST software. From the response of simulated Specific absorption rate, we analyzed the statistical differences between the normal head and the head that contains tumor. From these results we were able to accurately find the presence of tumour.

References

[1] B. J. Mohammed, A. M. Abbosh, S. Mustafa, and D. Ireland, "Microwave system for head imaging," Instrumentation and Measurement, IEEE Transactions on, vol. 63, pp. 117-123, 2014.

[2] o. N.-I. R. H. IEEE Standards Coordinating Committee 28, IEEE Standard for Safety Levels with Respect to Human Exposure to Radio Frequency Electromagnetic Fields, 3kHz to 300 GHz: Institute of Electrical and Electonics Engineers, Incorporated, 1992.

[3] A. Sabouni and A. Kishk, "Dual-polarized, broadside, thin dielectric Resonator antenna for microwave imaging," Antennas and Wireless Propagation Letters, IEEE, vol. 12, pp. 380-383, 2013.

[4] A. T. Mobashsher, A. M. Abbosh, and Y. Wang, "Microwave system to detect traumatic brain injuries using compact unidirectional antenna and wideband transceiver with verification on realistic head phantom," Microwave Theory and Techniques, IEEE Transactions on, vol. 62, pp. 1826-1836, 2014.

[5] X. Li, M. Jalilvand, Y. L. Sit, and T. Zwick, "A compact double-layer onbody matched bowtie antenna for medical diagnosis," Antennas and Propagation, IEEE Transactions on, vol. 62, pp. 1808-1816, 2014.

[6] A. T. Mobashsher and A. Abbosh, "Slot-loaded folded dipole antenna with wideband and unidirectional performance for L-band applications," Antennas and Wireless Propagation Letters, IEEE, vol. 13, pp. 798-801, 2014.

References

[7] S. Ahdi Rezaeieh and A. Zamani, "3-D Wideband Antenna for HeadImaging System with Performance Verification in Brain Tumor Detection," Antennas and Wireless Propagation Letters, IEEE, vol. 14, pp. 910-914, 2015.

[8] C. Chiu, H. Wong, and C. Chan, "Study of small wideband folded-patchfeed antennas," IET Microwaves, Antennas & Propagation, vol. 1, pp. 501-505, 2007.

[9] T. Taga and K. Tsunekawa, "Performance Analysis of a Built-In Planar Inverted F Antenna for 800 MHz Band Portable Radio Units," IEEE Journal on Selected Areas in Communications, vol. 5, pp. 921-929, 1987.

[10] W.-L. Chen, G.-M. Wang, and C.-X. Zhang, "Bandwidth enhancement of a microstrip-line-fed printed wide-slot antenna with a fractal-shaped slot," Antennas and Propagation, IEEE Transactions on, vol. 57, pp. 2176-2179, 2009.

[11] S. Ahdi Rezaeieh, A. Abbosh, and Y. Wang, "Wideband unidirectional antenna of folded structure in microwave system for early detection of congestive heart failure," Antennas and Propagation, IEEE Transactions on, vol. 62, pp. 5375-5381, 2014.

[12] C. M. Kruesi, R. J. Vyas, and M. M. Tentzeris, "Design and development of a novel 3-D cubic antenna for wireless sensor networks (WSNs) and RFID applications," Antennas and Propagation, IEEE Transactions on, vol. 57, pp. 3293-3299, 2009.

References

[13] S. Ahdi Rezaeieh, A. Zamani, and A. Abbosh, "3-D Wideband Antenna for Head-Imaging System with Performance Verification in Brain Tumor Detection," IEEE Antennas and Wireless Propagation Letters, vol. 14, pp. 910-914, 2015.

[14] K. Foster, J. Schepps, R. Stoy, and H. P. Schwan, "Dielectric properties Of brain tissue between 0.01 and 10 GHz," Physics in medicine and biology, vol. 24, p. 1177, 1979.

[15] S. Gabriel, R. Lau, and C. Gabriel, "The dielectric properties of biological tissues: II. Measurements in the frequency range 10 Hz to 20 GHz," Physics in medicine and biology, vol. 41, p. 2251, 1996.

[16] A. Peyman, S. Holden, S. Watts, R. Perrott, and C. Gabriel, "Dielectric properties of porcine cerebrospinal tissues at microwave frequencies: in vivo, in vitro and systematic variation with age," Physics in medicine and biology, vol. 52, p. 2229, 2007.

[17] M. Jalilvand, X. Li, L. Zwirello, and T. Zwick, "Ultra wideband compact near-field imaging system for breast cancer detection," IET Microwaves, Antennas & Propagation, 2015.

[18] R. K. Amineh, M. Ravan, A. Trehan, and N. K. Nikolova, "Near-field microwave imaging based on aperture raster scanning with TEM horn antennas," Antennas and Propagation, IEEE Transactions on, vol. 59, pp. 928-940, 2011.

References

[19] B. Menze et al., “The multimodal brain tumour image segmentation benchmark (brats),” IEEE Transactions on Medical Imaging, vol. 34, no. 10, pp. 1993–2024, 2015.

[20] Pereira, S., Pinto, A., Alves, V., et al.: ‘Brain tumour segmentation using convolutional neural networks in MRI images’, IEEE Trans. Med. Imaging, vol, 35, pp. 1240–1251,2016.

Thank You